# Invar Alloys: Information from the Study of Iron Meteorites

J. I. Goldstein, D. B. Williams, J. Zhang, and R. Clarke*

Department of Materials Science and Engineering,
Lehigh University, Bethlehem, PA

*Division of Meteorites, Smithsonian Institution,
Washington, D. C.

## ABSTRACT

The iron meteorites were slow cooled ($<10^8$ years) in their asteroidal bodies and are useful as indicators of the phase transformations which occur in Fe-Ni alloys. In the invar composition range, the iron meteorites contain a cloudy zone structure composed of an ordered tetrataenite phase and a surrounding honeycomb phase either of gamma or alpha phase. This structure is the result of a spinodal reaction below 350°C. The Santa Catharina iron meteorite has the typical invar composition of 36 wt% Ni and its structure is entirely cloudy zone although some of the honeycomb phase has been oxidized by terrestrial corrosion. Invar alloys would contain such a cloudy zone structure if more time was available for cooling. A higher temperature spinodal in the Fe-Ni phase diagram may be operative in invar alloys but has not been observed in the structure of the iron meteorites.

Physical Metallurgy of Controlled
Expansion Invar-Type Alloys
Edited by K.C. Russell and D.F. Smith
The Minerals, Metals & Materials Society, 1990

## Introduction

Invar alloys are based on the composition Fe-36 wt% Ni and have a near zero thermal expansion coefficient over a substantial temperature range. The anomalous thermal expansion property of invar alloys is accompanied by many other anomalies of various physical properties which have been found experimentally. The invar alloys are typically heat treated at 800°C for 1 hour and then rapidly cooled (McClintock and Argon, 1966)[12]. Presumably the unusual properties of invar alloys are obtained as a result of this heat treatment. The type of microstructure obtained is single phase and no microstructural or metastable phases have been identified. One of the ways in which we can study phase transformations which may be responsible for invar behavior is to investigate materials of similar composition which have been heat treated for very long periods of time in the same temperature range. Fortunately we have available in our laboratories iron meteorites which are Fe-Ni alloys and were cooled slowly after solidification in asteroidal bodies for millions of years.

The iron meteorites are Fe-Ni alloys which contain from 5 to 60 wt% Ni and small amounts (< 1 wt%) of Co, P, S, and C. Most of the P, S, and C are found in phosphides, sulfides, and carbides which form at relatively high temperatures. Iron meteorites are cooled slowly at rates from 5 to 500°C per million years in their parent asteroidal bodies (Saikumar and Goldstein, 1988).[18] These meteorites contain a range of microstructures (some phases which are at local equilibrium and some phases which are metastable) over a range of chemistry which may be useful in attempting to understand the microstructure of invar alloys. The purpose of this paper is to describe the meteorite structure/chemistry in the invar range and to extrapolate these findings in order to understand invar alloys.

## Fe-Ni Phase Diagram

Before we discuss the detailed structures that form in the invar composition range of the iron meteorites, we need to understand the currently available information on the Fe-Ni phase diagram. This phase diagram will serve as a guide to the phase transformations which occur on cooling. The Fe-Ni phase diagram from 900°C to about 400°C was recently determined by Romig and Goldstein (1980)[16] and is shown in Figure 1. The diagram looks remarkably simple with two major phases, alpha and gamma, and a two phase alpha plus gamma region. Using the Romig and Goldstein phase diagram, for a typical invar alloy, heat treatment at 800°C occurs in the gamma phase. The alloy would enter the two phase region at about 450°C during the cooling process.

Experimentally, the alpha phase can not be nucleated directly in Fe-Ni alloys without first forming martensite. In order to determine the Fe-Ni phase diagram then, Romig and Goldstein reheated alloys from low temperature martensite into the two phase alpha and gamma region and measured tie line compositions using the electron probe microanalyzer (EPMA) or the analytical electron microscope (AEM). It is important to note that no attempt was made to heat treat alloys above the gamma/ alpha + gamma two phase boundary to measure the presence of any equilibrium or non equilibrium phase. These authors assumed that Fe-Ni alloys (including invar alloys) are single phase gamma above the two phase boundary. Recently, microscopic evidence for a spinodal-type phase separation in a number of neutron or heavy ion irradiated Fe-Ni and Fe-Ni-Cr invar alloys over a temperature range of 425 to 650° C has been observed (Russell and Garner, 1989).[17] Clearly these recent data are important in developing pertinent phase diagram information for invar alloys and conflict with

current information about the Fe-Ni phase diagram based on binary alloys.

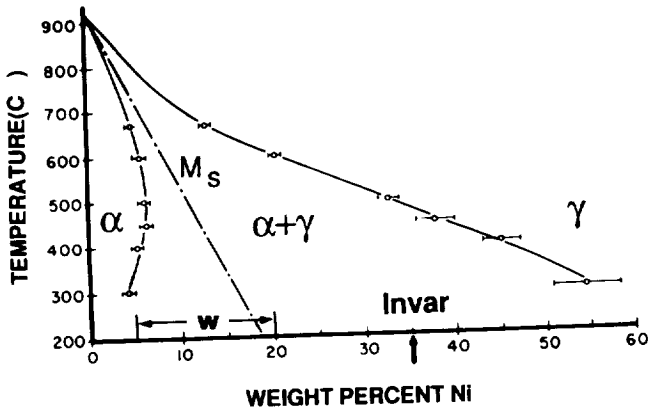


Figure 1. Fe-Ni phase diagram (Romig and Goldstein, 1980)[16]. The error bars indicate the uncertainty in the tie line composition of the two equilibrium phases, alpha and gamma. The vertical line indicates the nominal invar alloy composition. The region between 5 and 20 wt% Ni, as marked (W) on the phase diagram, is the Ni composition range of the iron meteorites which have developed a Widmanstatten pattern.

The low temperature portion of the Fe-Ni phase diagram has recently been revised based on both meteoritical evidence (Reuter et al, 1989a)[14] and electron irradiation of laboratory Fe-Ni alloys (Reuter et al, 1989b)[15], Figure 2. The authors concentrated on the composition range from 0 to 50 wt% Ni and on temperatures below 400°C. Both the stable and metastable phase boundaries are defined. They observed an asymmetrical miscibility gap which is metastable below 390°C and is caused by the presence of a tricritical point which is produced by magnetic interactions. Within the miscibility gap there is the expected asymmetrical spinodal decomposition region. The eutectoid at 390°C and the miscibility gap and associated tricritical point at 462°C and 48.9 wt% Ni were predicted by Chuang et al (1986)[2] using thermodynamic calculations which took into account the magnetic contribution to the Gibbs free energy of the low Ni, body-centered cubic phase and the high Ni, face-centered cubic phase. The tricritical point separates the paramagnetic $gamma_1$ from the ferromagnetic $gamma_2$. The Curie temperature ($T_c^{\gamma}$) is shown on Figure 2 and is extended to low temperatures using the calculations of Chuang et al (1986).[2]

Reuter et al (1989a)[14] used observations of iron meteorite structures to determine the equilibrium between the low Ni, alpha phase, and ordered FeNi. The slow Ni diffusion rates below 350°C precluded the use of experimental alloys for this measurement. In addition, electron irradiation experiments were carried out in the high voltage electron microscope in order to determine the temperature at which the ordered FeNi phase was formed in laboratory Fe-Ni alloys ranging in Ni content from 32 wt% to 50 wt% (Reuter et al, 1989b).[15] To complete the phase diagram, the

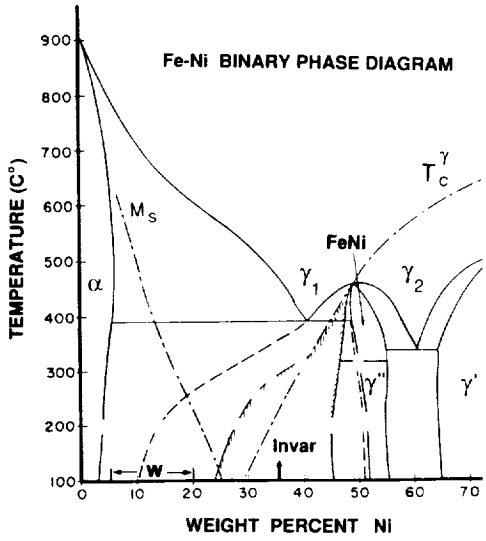


Figure 2. Low temperature portion of the Fe-Ni phase diagram (Reuter et al, 1989)[14, 15]. The equilibrium and metastable phase boundaries are shown. See text for definitions of the various boundaries and phase fields. The vertical line indicates the nominal invar alloy composition. The region between 5 and 20 wt% Ni, as marked (W) on the phase diagram, is the Ni composition range of the iron meteorites which have developed a Widmanstatten pattern.

martensite start temperature $M_s$ is included and the $FeNi_3$ region (gamma') is drawn for completeness although it was not specifically measured by Reuter et al (1989a)[14].

One can apply the phase diagram of Reuter et al (1989a)[14], Figure 2, directly to invar alloys of 36 wt% Ni. Gamma phase is assumed to be stable to about 450°C. Below about 450°C one would expect the equilibrium alpha and $gamma_1$ phases to be present in the alloy. However, as stated before, the alpha phase can not be nucleated directly in binary Fe-Ni alloys without first forming martensite. Therefore it is likely that nucleation and growth of alpha in invar alloys will be suppressed. When the alloy enters the miscibility gap below 400°C, the nucleation of Ni-poor $gamma_1$ and FeNi (gamma") is also likely to be suppressed until the alloy enters the spinodal region where no barrier exists to the transformation. Spinodal decomposition is predicted to occur just above 300°C with the two products being metastable, supersaturated paramagnetic $gamma_1$ and ordered FeNi. These two phases have varying compositions depending on the lowest heat treatment temperatures. When the temperature falls below about 250°C, where the miscibility gap crosses $M_s$, the $gamma_1$ phase will transform to bcc martensite (See Figure 2). Because the martensite transformation is diffusionless, and athermal, it will occur below 250°C, despite the very slow Ni diffusion rates.

## Structures of Iron Meteorites

Over 98% of the more than 500 known iron meteorites have Ni contents which lie between 5 and 20 wt % Ni (Buchwald, 1975).[1] This composition range is plotted on the Fe-Ni phase diagram of Romig and Goldstein (1980)[16], Figure 1, and the Fe-Ni phase diagram of Reuter et al (1989a)[14], Figure 2, along with the nominal composition of invar alloys, 36 wt% Ni. Although the vast majority of the iron meteorites do not have the invar composition, gradients with Ni contents exceeding 50 wt% develop in the parent gamma phase as the Widmanstatten pattern of alpha plates in a gamma matrix grows at low temperatures. The nominal invar composition is included in the Ni composition gradient and that Ni content goes through a spinodal phase transformation at lower cooling temperatures. These transformations will be described in detail in the section which follows.

There is one iron meteorite, Santa Catharina, which has the nominal composition of the invar alloy. This meteorite has cooled directly without forming a Widmanstatten structure. The detailed structure which formed on cooling will discussed later in the paper. Unfortunately the structure of Santa Catharina is masked in part by terrestrial oxidation which makes interpretation of the structure non trivial.

## Widmanstatten Pattern

The vast majority of the iron meteorites which contain between 5 and 20 wt % Ni are single crystal gamma, fcc, at high temperatures and cool slowly in their parent bodies. As cooling continues, alpha nucleates from gamma (see Figure 1) in the temperature range from 750 to 600$^{o}$C and a Widmanstatten pattern begins to develop. As cooling continues, alpha and gamma both increase in Ni and alpha grows at the expense of gamma. Below 400$^{o}$C the development of the Widmanstatten pattern follows the Fe-Ni phase diagram developed by Reuter et al (1989a)[14], Figure 2. Figure 3a shows a typical Widmanstatten pattern which develops, in this case in the Dayton iron meteorite (17.6 wt% Ni, 0.4 wt% P, Buchwald, 1975)[1]. It should be noted, that although the development of the Widmanstatten pattern has not been reproduced in the laboratory for binary Fe-Ni alloys, it has been reproduced in ternary Fe-Ni-P alloys with the same alloy compositions as the iron meteorites (Narayan et al, 1985).[11] The phase diagram of Fe-Ni-P has been obtained by directly cooling ternary alloys into the alpha plus gamma region (Romig and Goldstein, 1980)[16] while the phase diagram of Fe-Ni first requires the formation of martensite. It appears, therefore, that the equilibrium gamma to alpha plus gamma transformation responsible for the gross Widmanstatten structure (Figure 3a) can only be nucleated by the presence of phosphorus. Phosphorus and phosphide precipitates are not present in invar alloys, and these alloys do not show the classic Widmanstatten pattern either. However, in this paper we will assume that P does not influence the phase transformations in which the invar structure is produced. This assumption is discussed later in this paper.

As cooling occurs, the diffusion coefficient of Ni decreases, for example, from $1.5 \times 10^{-16}$ cm$^2$/sec at 700$^{o}$C to $1 \times 10^{-21}$ cm$^2$/sec at 500$^{o}$C. At lower temperatures diffusion cannot keep up with the mass transport required. A Ni build-up then develops in the gamma phase close to the alpha/gamma boundary. In this scenario, chemical equilibrium as dictated by the Fe-Ni phase diagram is maintained between alpha and gamma only at the alpha/gamma boundary. The rest of the structure is metastable. Figure 3b shows such a Ni profile, measured with the EPMA, which has developed in the Grant meteorite cooled at the rate of ~ 10$^{o}$C per million years.

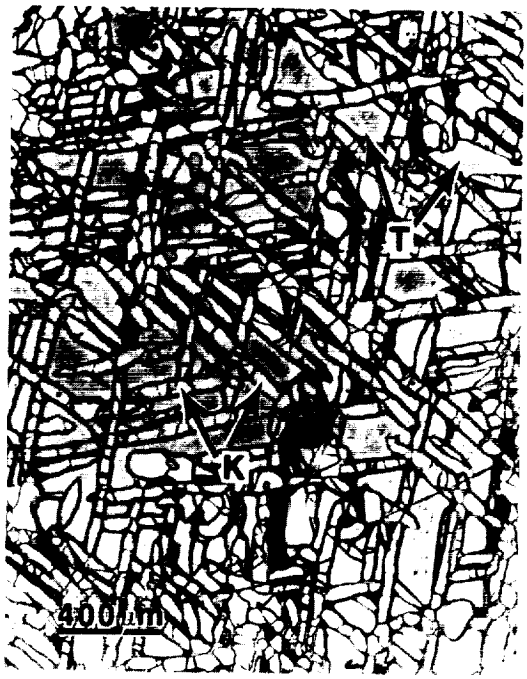


Figure 3a. Light optical micrograph of a typical Widmanstatten pattern which develops in iron meteorites. This meteorite is the Dayton iron meteorite which contains 17.6 wt% Ni, 0.4 wt% P (Buchwald, 1975)[1].

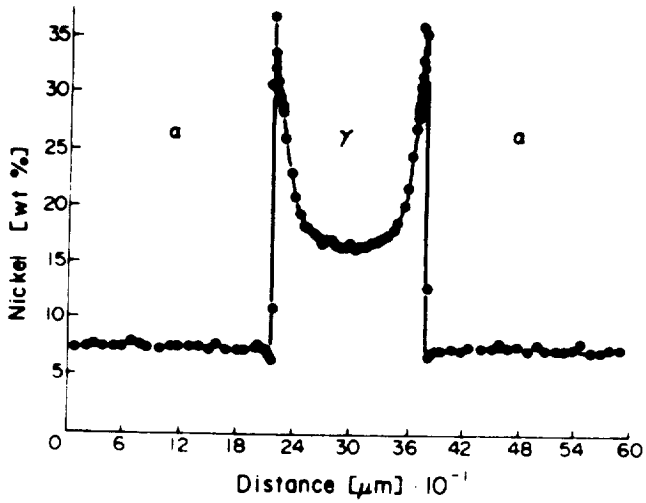


Figure 3b. Ni concentration gradient across an alpha-gamma-alpha area in the Grant meteorite taken with the electron probe microanalyzer. This meteorite cooled at the rate of approximately 10°C per million years.

Figure 4 shows a set of calculated Ni composition profiles as a function of temperature for a nominal 17 wt% Ni meteorite with a cooling rate of 50°C per million years (Reuter et al, 1988).[13] A Crank-Nicholson explicit finite difference model with variable grid spacing was used for the calculation (Saikumar, 1988)[18] and included the most recent diffusion coefficients measured for the temperature range 800-500°C (Dean and Goldstein, 1986)[6] and the phase boundaries of the newly determined Fe-Ni phase diagram (Reuter et al, 1989a).[14] The zero point on the distance axis represents the center of the alpha phase. The Widmanstatten alpha phase grows into the gamma phase as temperature decreases and the final half width is about 29 microns. Following the Ni profiles as the meteorite cools, one can observe that below 500°C, diffusion cannot keep up with the mass transport required to maintain long range equilibrium. At this temperature the gamma side of the alpha/gamma interface has about 28 wt% Ni. The invar composition of 36 wt% Ni appears on the gamma side of the alpha/gamma interface between 450 and 400°C. As a result of the diffusion process in gamma, the invar composition of 36 wt% Ni is present in the gamma phase and moves over a micron away from the alpha/gamma interface into the gamma at 350°C and below. The Ni gradient which has developed above 350°C is retained to low temperatures because of the low Ni diffusion coefficient. Such a Ni gradient is shown in Figure 3b taken with the EPMA. Any decomposition that occurs below 350°C results in a microstructure that is on the sub micron scale. Below 350°C, the invar composition is retained and enters the miscibility gap below the eutectoid, Figure 2. Clearly, it is this part of the meteorite microstructure which we must focus on.

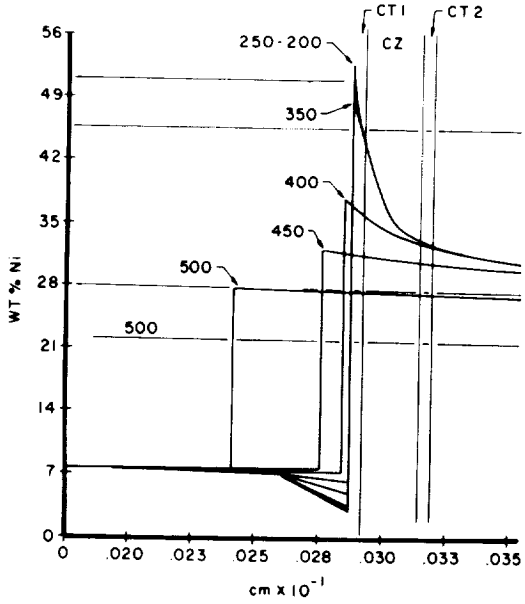


*Figure 4.* Calculation of Ni composition profiles during Widmanstatten pattern growth in a meteorite with a bulk Ni content of 17 wt% Ni, 0.4 wt% P and a cooling rate of 50°C per million years (Reuter et al, 1988)[13].

The structures and compositions of the original gamma phase near the alpha/gamma interface can be summarized in the transmission electron micrograph, Figure 5 and the composition profile, Figure 6. The details of these figures are beyond the scope of this paper (See Reuter et al, 1988)[13] but briefly it is possible to relate the four regions in Figure 5 to the Fe-Ni phase diagram in Figure 2 by drawing a line across the diagram at approximately 200°C, a temperature below which Ni diffusion ceases, even in meteorites. The equilibrium phases are alpha (4 wt% Ni) and ordered FeNi (approximately 52 wt% Ni) shown by the solid lines in Figure 2 and present at the K/CT 1 interface in Figure 5. The miscibility gap (dashed lines) composition range (11 wt % Ni to 51 wt% Ni) spans the composition range of the two phase structure labeled CZ in Figure 5. This region is known as the 'cloudy zone' because of its appearance in low magnification optical micrographs. Its fine two-phase structure is revealed in TEM micrographs as shown in Figure 7. The composition of the globular phase is about 51 wt% Ni and the phase is ordered FeNi with an $L1_0$ superstructure. The composition of the honeycomb phase is difficult to establish because it is so narrow (< 0.1 um) but is about 12 wt% Ni, for example in the very slow-cooled, coarse structure in the Estherville meteorite. The structure of the honeycomb phase in the meteorites studied by Reuter et al (1988)[13] is body centered cubic, martensite. The average composition of the cloudy zone two-phase structure varies from about 46 wt% Ni at the CZ/CT-1 interface to roughly 30 wt% Ni at the CZ/CT-2 interface. As shown in Figure 5, the size of the ordered FeNi globular phase in the CZ decreases in size from the CT-1 interface to the CT-2 interface. The region between the $M_S$ line and the spinodal (hatched line) in Figure 2 represent the CT-2 region in Figure 5 which is supersaturated gamma, unable to transform by nucleation and growth. The spinodal line compositions correspond to the bulk composition range in which the CZ forms.


Figure 5. A transmission electron microscope bright field image of an alpha-decomposed gamma region in the Tazewell iron meteorite (16.9 wt% Ni). The regions which are observed are K - alpha, CT-1 - clear taenite, CZ - cloudy zone, CT-2 - clear taenite 2. A martensite phase occurs at lower Ni contents next to the CT-2 (Reuter et al, 1988)[13].

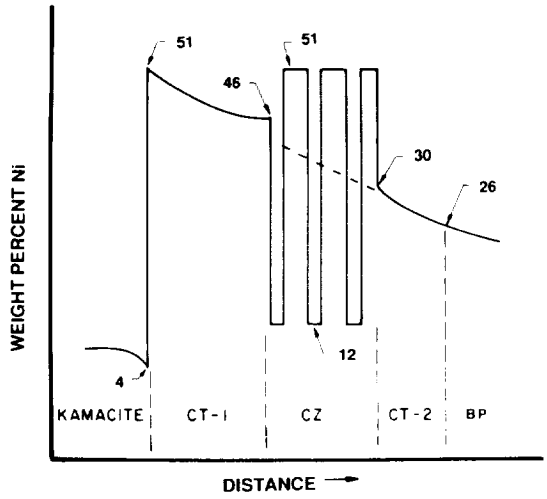


Figure 6. A schematic representation of the chemical composition of the structures in the gamma region near the alpha-gamma phase boundary as determined by x-ray analysis in the analytical electron microscope (Reuter et al, 1988)[13].

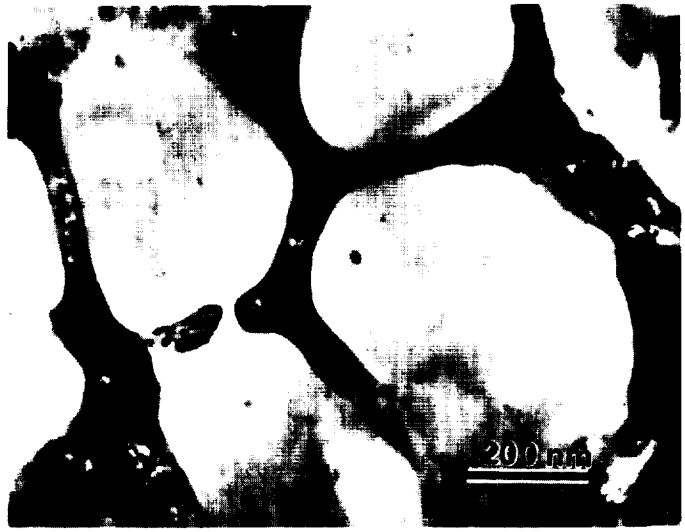


Figure 7. A transmission electron microscope bright field image of the cloudy zone (CZ) in the Estherville mesosiderite. The globular phase is FeNi and is surrounded by a honeycomb phase of lower Ni content (Reuter et al, 1988)[13].

The invar composition falls in the middle of the cloudy zone composition range, coincident with the miscibility gap / spinodal decomposition area of Figure 2, so we should examine this part of the structure in more detail. The part of the meteorite with the invar composition decomposes spontaneously, producing Ni rich and Fe rich regions defined by the miscibility gap. At 300°C for example, the region containing the highest Ni content, about 41 wt% Ni, spinodally decomposes into Ni-rich gamma , FeNi, containing 51 wt% and Ni-poor $gamma_1$ containing 26 wt%. Depending on the cooling rate and therefore the time available for diffusion below 300°C, the Ni content of the Ni poor $gamma_1$ region may or may not decrease in Ni content as the temperature decreases. If the Ni content in $gamma_1$ remains above 25 wt% Ni, gamma is retained as the honeycomb phase in the final structure of the cloudy zone. If the Ni content of $gamma_1$ is less than about 25 wt% Ni, this phase transforms to martensite, which becomes the honeycomb phase of the cloudy zone.

In summary, the development of the Widmanstatten structure in the vast majority of iron meteorites leads to the build up of Ni in the parent gamma phase of the meteorite. This build up contains the nominal invar composition of 36 wt% Ni which enters the gamma phase between 450 and 400°C. The invar composition is retained below temperatures of 350°C where a spinodal decomposition occurs producing the cloudy zone, a structure containing ordered FeNi and a matrix of body centered cubic martensite. This cloudy zone structure is present in all iron meteorites which display a Widmanstatten structure except those where shock reheating above 500°C has occurred. Clearly nominal invar alloys should display the cloudy zone structure at some stage of development when heat treated at 300°C or below. However it should be noted that this scenario for invar structure formation, which is based on the development of the structure of the Widmanstatten pattern in iron meteorites, is only valid if no reactions take place at the annealing temperature of 800° C or during cooling of the invar alloy to the range of 450 to 400° C. If such reactions take place, then the cloudy zone structure will most likely be super imposed on the high temperature microstructure.

Invar Composition Meteorites

There are two iron meteorites with more than 27 wt% Ni, Twin City and Santa Catharina, which have been cooled directly from high temperatures, >800°C. These iron meteorites do not have a Widmanstatten pattern and alpha, body centered cubic, is only present in small amounts. We will summarize structural and chemical data available to date and relate this information to the development of structure in invar composition alloys.

Santa Catharina is an anomalous nickel and sulfur rich iron meteorite. Its metal composition is highly variable. For example our sample from the British Museum (BM#52283) contains 27 to 29 wt% Ni while our sample from the US National Museum (USNM#3043) contains around 35 to 36 wt% Ni. Both these samples contain phosphides. Since almost all studies to date have been carried out on samples similar to the high Ni USNM#3043, we will describe that sample in some detail. It contains 35.3 wt% Ni and 0.2 wt% P and shows no trace of Widmanstatten precipitation (Buchwald, 1975).[1] The meteorite is polycrystalline and the grains are separated by sulfide (FeS) veins. No alpha phase is present except for small 1-3 micron rims around the phosphides (Buchwald,1975[1], Clarke,1984[3]). Oxidation has also attacked the gamma matrix which makes examination of the surface difficult (Buchwald, 1975).[1] As discussed earlier in this paper, one would predict from the Fe-Ni phase diagram (Figures 1 and 2) and from the results of the TEM and AEM investigations of gamma in lower Ni iron meteorites that invar

alloys and meteorites at the nominal 36 wt% Ni range would have a cloudy zone microstructure. This prediction assumes that P does not have a special effect on meteorite microstructures apart from aiding nucleation of the Widmanstatten structure and that no spinodal type reaction occurs in the gamma region above 450°C in the binary Fe-Ni phase diagram.

The general microstructure of the high Ni Santa Catharina specimen is shown by the light optical microscopy (LOM) and backscattered electron (BSE) micrographs of the metal areas (Figure 8). The specimen was lightly etched with nital for LOM observation. Two regions, one light and one dark, are recognizable on the micrographs. The dark regions in the LOM image are also dark in the BSE image. The atomic number contrast available in the BSE images shows clearly that the dark region has a lower average atomic number than the light region. Lovering and Andersen (1965), using the electron probe microanalyzer (EPMA), showed that the light region contains 31.8 wt% Ni, <0.1 wt% P, and no detectable oxygen. The dark region contains about equal amounts of Fe and Ni (46.1 wt% Fe, 45.2 wt% Ni), <0.1 wt% P, and 8.4 wt% O. We have confirmed these analyses with our specimen of USNM#3043 using EPMA although we find more Ni, 34.9 wt % Ni, in the light regions. This Ni composition places the light-metal region in the cloudy zone range. We conclude that the dark region has a lower atomic number because it contains an oxide phase. Lovering and Andersen (1965)[9] and Clarke (1984)[3] argue that the dark region was selectively oxidized by terrestrial oxidation along cracks.

Figure 8a. Light optical micrograph of an etched sample of the Santa Catharina meteorite (Sample USNM #3043). A light and a dark region are recognizable on the micrograph. A large phosphide in the approximate center of the micrograph is surrounded by a light (metal) region.

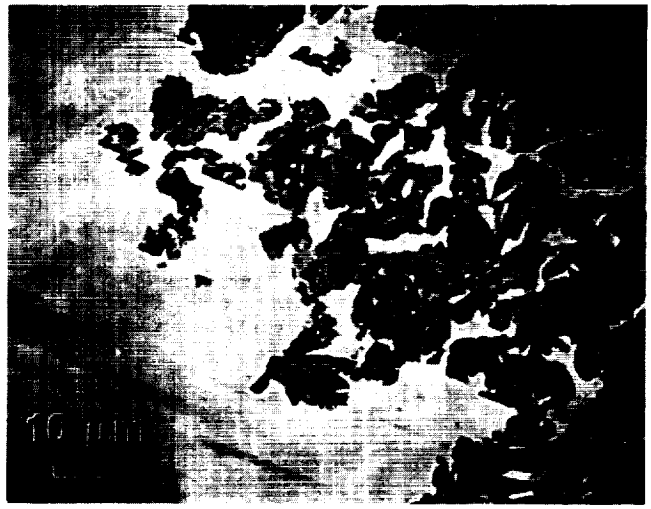

Figure 8b. Back scattered electron image of a polished section of the Santa Catharina meteorite (Sample USNM #3043). The dark regions in this micrograph have a lower atomic number than the light (metal) regions.

Figure 9 shows a LOM of the light and dark regions at higher magnification. The light region is filled with small aligned phosphides. In addition, the light metal region, when etched, turns mostly brown. The brown contrast is very similar to that observed when the cloudy zone in the gamma phase of the iron meteorites is chemically etched. This suggests that the unoxidized light metal area with a composition of approximately 35 wt% Ni contains at least some type of cloudy zone structure.

Mossbauer investigations have also been carried out on the Santa Catharina meteorite. This technique can determine the structure of the phases present in the meteorite. However the analysis is made on millimeter or larger regions of the sample so no correlation can be made between the microstructure on the sub millimeter scale and the results of the measurement. In most cases, both light and dark regions were analyzed at the same time. Jago (1982) used Mossbauer techniques and found two phases in the meteorite, a ferromagnetic ordered FeNi and a paramagnetic disordered gamma. These results were very similar to those of Lovering and Parry (1962) who used a thermomagnetic analysis technique and found similar type phases. Danon et al (1979) used Mossbauer techniques and also measured a FeNi ordered phase with a $L1_0$ superstructure and a paramagnetic phase of approximately 27 wt% Ni. They attempted to correlate the Mossbauer results and the microstructure of the meteorite and incorrectly identified the dark regions as FeNi and the light regions as the iron rich paramagnetic phase. Scorzelli and Danon (1985) reconfirmed the previous Mossbauer results on Santa Catharina and also used the EPMA to reconfirm the local chemical analysis of the dark and light regions. Unfortunately

they still consider each region as a separate phase. This illustrates the problem of interpreting data from a technique that samples large areas of the specimen.

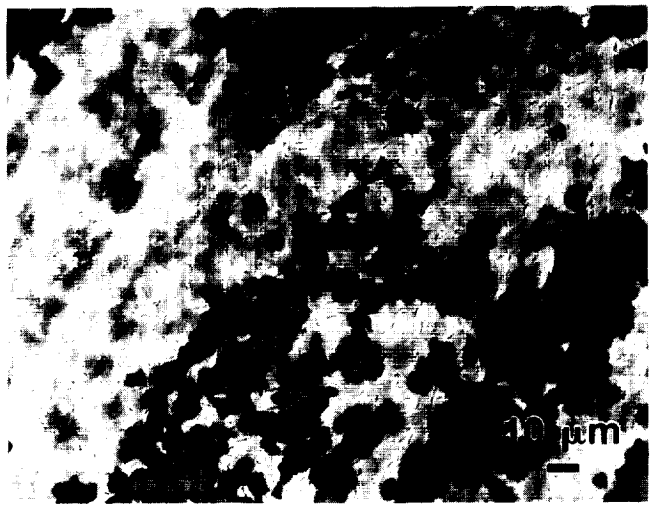


Figure 9. Light optical micrograph of an etched sample of the Santa Catharina meteorite (Sample USNM #3043) at higher magnification showing the light and dark regions in more detail. The light region is filled with small aligned phosphides.

Jago (1979[7],1982[8]) has used the TEM to investigate the structure of the high-Ni Santa Catharina meteorite. His TEM photograph shows a cloudy zone in the dark region. Furthermore, Jago (1979)[7] states that cloudy zone is present in both the light and dark regions with a very small particle size in both regions (~ 10nm). His electron diffraction work suggests coexisting gamma phases in the cloudy zone which is in conflict with the structure for cloudy zone, ordered gamma FeNi and alpha, martensite observed by Reuter et al (1988)[13] for several lower Ni meteorites. Jago was also the first to suggest that spinodal decomposition is the precursor for the cloudy zone structure as confirmed in later investigations (Reuter,1988)[13].

Figure 10 shows a TEM bright field image of the high Ni Santa Catharina meteorite which includes both the dark oxide-containing region and the light metal containing region. The existence of both these regions was confirmed by x-ray EDS analysis of Fe-Ni. In addition, electron energy loss analysis confirms the presence of oxygen in the dark region. A cloudy zone structure with a size range of approximately 20nm is observed. The cloudy zone structure of the metal-containing area has a much lower contrast. We have observed that in the dark oxide area there is an ordered fcc phase (FeNi) and an oxide phase, probably $Fe_2NiO_4$, which constitutes

the honeycomb structure. Jago (1979)[7] stated that there are two fcc phases in the light metal regions, one of which is ordered FeNi. Unfortunately no evidence of this finding was given in his paper. The FeNi phase form the islands in the structure and the second fcc phase forms the honeycomb phase. From these observations we propose that the entire sample of Santa Catharina had this type of cloudy zone structure originally and that the low Ni phase was preferentially corroded forming the oxide in the dark regions.

The low Ni sample of Santa Catharina (BM#52283) contains 27 to 29 wt% Ni. Figure 11 shows a LOM image of the sample. Aligned phosphides are present throughout the metal matrix. TEM analysis shows the presence of an ordered phase, probably FeNi, about 10 nm in size in a matrix of fcc gamma. This structure is very similar to that of the Twin City iron meteorite which contains 29.4 wt% Ni (Reuter et al, 1988)[13]. In addition both meteorites contain precipitates of alpha, bcc, although the size of the alpha phase is smaller in Santa Catharina. The alpha phase in both meteorites does not form a Widmanstatten pattern. Danon and Scorzelli (1985) also studied a large area of well preserved metal (non oxidized) of approximately 30 wt% Ni in the Santa Catharina meteorite using conversion electron Mossbauer spectroscopy. This specimen of Santa Catharina is probably very similar to our BM #52283 sample. They found almost equal amounts of ordered ferromagnetic FeNi, paramagnetic gamma, and alpha. Combining results of Mossbauer, x-ray diffraction, and TEM they argue, as we do, that the large preserved metal area is virtually all cloudy zone composed of ordered FeNi and a lower Ni paramagnetic gamma. It is clear that both the low Ni Santa Catharina sample and the Twin City meteorites cooled slowly and entered the two phase alpha plus gamma region in the Fe-Ni phase diagram at a much lower temperature than in almost all iron meteorites. The presence of an ordered fcc phase in a fcc matrix indicates that spinodal decomposition occurs upon cooling even in Fe-Ni alloys below the nominal invar composition.

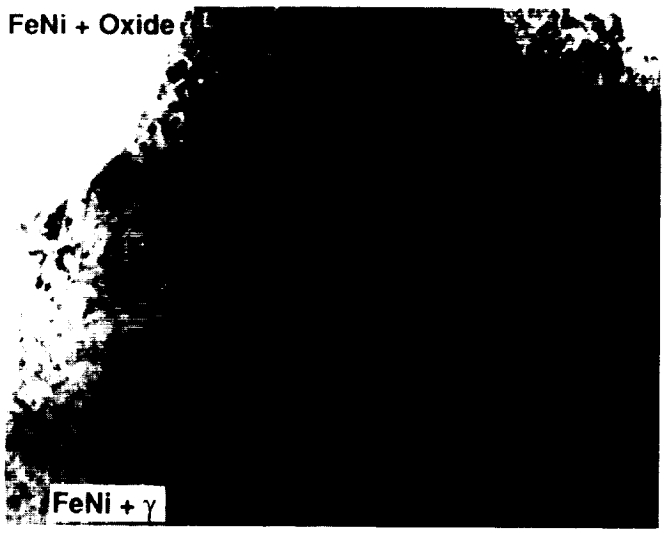


Figure 10. Transmission electron microscope bright field image of the Santa Catharina meteorite (Sample USNM #3043) showing both dark and light regions. A cloudy zone structure is observed in both regions.

Figure 11. Light optical micrograph of a low Ni (27 to 39 wt% Ni) sample of the Santa Catharina meteorite (BM #52283). Aligned phosphides are present throughout the metal matrix.

In summary, our results on Invar composition meteorites show that they form a cloudy zone upon slow cooling. The cloudy zone is different to that observed in several meteorites by Reuter et al (1988)[13] in that the honeycomb phase is gamma. In addition the cloudy zone is much smaller, 10 to 20 nm rather than 100 to 500 nm (Reuter et al, 1988)[13]. These invar composition meteorites form the cloudy zone directly upon cooling rather than by developing the invar composition first at temperatures below 450°C during the formation of the Widmanstatten pattern. All the meteorite cloudy zone structures studied by Reuter et al (1988)[13] formed by the later process. The results of the study of Invar composition meteorites indicate that the spinodal decomposition occurred below about 350°C as indicated by the Fe-Ni phase diagram (Reuter et al, 1989a)[14]. Spinodal decomposition proposed by Russell and Garner (1989)[17] which occurs above 450°C will produce a much larger spinodal, one on the micron size level. This spinodal size is much larger than that observed in Santa Catharina.

## Discussion

1. Cloudy Zone - The evidence from the iron meteorites clearly indicates that regions of these meteorites containing 36 wt% Ni (invar composition range) form a cloudy zone structure. This structure is believed to form by spinodal decomposition below 350°C during cooling of the iron meteorites. The slow cooling history of the iron meteorites is responsible for the size of the structure which allows us to observe the

cloudy zone structure in the analytical electron microscope. Since the invar alloys cool through this temperature range (<350°C), it might be expected that these alloys adopt the same structure although on a much smaller scale, one that might not be easily observed using electron microscope, x-ray or other techniques.

2. Size of the cloudy zone - The growth of the cloudy zone in meteorites takes place over millions of years. It might be of interest to speculate what would happen if the cooling rate was less than an hour. If we assume growth is a function of $t^{1/2}$, then we can obtain a first order calculation. Since a million years is approximately $10^{10}$ times longer that an hour, we should have about $10^{-5}$ less growth if the growth process was diffusion controlled. In the Santa Catharina meteorite, the cloudy zone is approximately 10 - 20 nm in size. Using the faster cooling rate of invar alloys we would calculate that any cloudy zone in the invar alloys is well below atomic (angstrom) dimensions. The spinodal reaction would at best be in its initial stages of formation. This calculated size range is consistent with the fact that the cloudy zone structure is not observed in invar alloys.

3. There is clear microscopic evidence for a spinodal-type phase separation in a number of neutron or heavy ion irradiated Fe-Ni and Fe-Ni-Cr invar alloys over a temperature range of 650°C to 425°C (Russell and Garner,1989)[17]. In Santa Catharina which cooled through this temperature range there is no structural or chemical evidence of the presence of this spinodal type phase separation. With the cooling rates typical of iron meteorites, this high temperature spinodal should grow to micron size in Santa Catharina (Russell and Garner, 1989[17]). The lack of this micron sized structure in Santa Catharina provides evidence that the equilibrium phase diagram was still controlling at these temperatures and that the low temperature spinodal formed due to the lack of equilibrium at low temperatures. However, the lack of the high temperature spinodal in the Santa Catharina meteorite does not prove that the reaction would not be operable in the faster cooling invar alloys. It should also be pointed out that low Ni (<30 wt%) iron meteorites which constitute over 98% of the iron meteorites do not reach invar composition in the gamma phase until they cool below 450°C. Therefore these meteorites do not have a thermal history which would allow the high temperature spinodal of Russell and Garner to influence their microstructure.

4. The most significant difference between iron meteorite and invar alloy compositions other than the Ni content is the presence of P. Phosphorus influences the nucleation of alpha allowing it to form directly upon cooling of Fe-Ni alloys (Narayan and Goldstein,1985)[11], to decrease the nucleation temperature of alpha phase in invar composition alloys over 50°C (Romig and Goldstein, 1980)[16], and to increase the diffusion coefficients in the gamma phase (Dean and Goldstein, 1986)[6] at temperatures as low as 500°C. At this time there is no information of the influence of P on the development of the cloudy zone or the effect of P on the phase transformations or phase diagrams below 400°C. In this paper we have assumed that the solubility of P is so low (<0.004 wt% P at 400°C) that all the P is in phosphides and it no longer influences the phase transformations in this temperature range. One piece of evidence which helps back this assumption is that the calculated eutectoid compositions at 390°C in the Fe-Ni system are the same as those measured in the iron meteorites (Reuter et al, 1988)[13]. The spinodal decomposition process involves no nucleation barrier, so the role of phosphorus in aiding nucleation of alpha is not relevant during cloudy zone formation, even if there is any P remaining in solution. If P remains in solution, it may

help the kinetics of cloudy zone formation making the structure coarser than if no P were present, but it would not effect the thermodynamics of the cloudy zone formation.

## Summary

The iron meteorites were slow cooled in their asteroidal bodies for millions of years and are useful as indicators of the phase transformations which occur in Fe-Ni alloys. In the invar composition range, the iron meteorites contain a cloudy zone structure composed of an ordered tetrataenite phase and a surrounding honeycomb phase either of gamma or alpha phase. This structure is the result of a spinodal reaction below 350$^{o}$C. The Santa Catharina iron meteorite has the typical invar composition of 36 wt% Ni and its structure is entirely cloudy zone although some of the honeycomb phase has been oxidized by terrestrial corrosion. If more time was available for cooling of invar alloys, these materials would contain such a cloudy zone structure. The cooling rate of the invar alloys is so fast that the cloudy zone structure cannot be detected in these alloys. A higher temperature spinodal in the Fe-Ni phase diagram may be operative in invar alloys but has not been observed in the structure of the iron meteorites.

## Acknowledgments

We wish to thank Dr. Ken Russell of the Massachusetts Institute of Technology for numerous technical discussions on the pertinent phase transformations. The support of NASA through Grant NAG -9-45 is gratefully acknowledged.

## References

(1) Buchwald V. F. (1975) Handbook of Iron Meteorites, their History, Distribution, Composition and Structure, Univ. California Press.

(2) Chuang Y. Y.,Chang Y. A., Schmid R. and Lin J. C. (1986) Magnetic contribution to the thermodynamic functions of alloys and the phase equilibria of the Fe-Ni system below 1200$^{o}$K. Met. Trans, 17A, 1361-1372.

(3) Clarke R. (1984) Structural development in the Santa Catharina meteorite. Meteoritics, 19, 207-208.

(4) Danon J., Scorzelli R. B., and Galvao da Silva, E. (1985), Microstructure of the Santa Catharina meteorite. Meteoritics 20, 632.

(5) Danon J., Scorzelli R., Souza Azevedo I., Curvello W., Albertsen J. F., and Knudsen J. M. (1979) Iron-nickel 50-50 superstructure in the Santa Catharina meteorite. Nature 277, 283-284.

(6) Dean D. C. and Goldstein J. I. (1986) Determination of the interdiffusion coefficients in the Fe-Ni and Fe-Ni-P systems below 900$^{o}$C. Met Trans. 17A, 1131-1138.

(7) Jago R. A. (1979) Santa Catharina and the origin of cloudy taenite in meteorites. Nature 279, 413-415.

(8) Jago R. A., Clark P. E., and Rossiter P. L. (1982) The Santa Catharina meteorite and the equilibrium state of Fe-Ni alloys. Phys. Stat. Sol. 74, 247-254.

(9) Lovering J. F. and Andersen C. A. (1965) Electron microprobe analysis of oxygen in an iron meteorite. Science 147, 734-736.

(10) Lovering J. F. and Parry L. G. (1962) Thermomagnetic analysis of co-existing nickel-iron metal phases in iron meteorites and the thermal histories of the meteorites. Geochim. Cosmochim. Acta 26, 361-382.

(11) Narayan C. and Goldstein J. I. (1985) A major revision of iron meteorite cooling rates- An experimental study of the growth of the Widmanstatten pattern. Geochim. Cosmochim. Acta 49, 397-410.

(12) McClintock F. A. and Argon A. S. (1966) ed. "Mechanical Behavior of Materials", Addison-Wesley Pub. Co., Inc. (Reading, MA), 202.

(13) Reuter K. B., Williams D. B., and Goldstein J. I. (1988) Low temperature phase transformations in the metallic phases of iron and stony-iron meteorites. Geochim. et Cosmochim. Acta, 52, 617-626.

(14) Reuter K. B., Williams D. B., and Goldstein J. I. (1989a) Determination of the Fe-Ni phase diagram below 400°C Met Trans, in press.

(15) Reuter K. B., Williams D. B., and Goldstein J. I. (1989b) Ordering in the Fe-Ni system under electron irradiation, Met Trans, in press.

(16) Romig A. D. and Goldstein J. I. (1980) Determination of the Fe-Ni-P phase diagrams at ion temperatures (700 to 300°C), Met. Trans. 11A, 1151.

(17) Russell K. C. and Garner F. A. (1989) High temperature phase separation in Fe-Ni and Fe-Ni-Cr invar-type alloys, submitted to Acta Met.

(18) Saikumar V. and Goldstein J. I. (1988) An evaluation of the methods to determine the cooling rates of iron meteorites. Geochim. Cosmochim. Acta 52, 715-726.

(19) Scorzelli R. B. and Danon J. (1985) Mossbauer spectroscopy and x-ray diffraction studies of Fe-Ni order-disorder processes in a 35% Ni meteorite (Santa Catharina). Physica Scripta. 32, 143-148.